Journal of Heredity 2011:102(S1):S40–S46
doi:10.1093/jhered/esr048

Identification of Risk Loci for Necrotizing Meningoencephalitis in Pug Dogs

Renee M. Barber, Scott J. Schatzberg, Jason J. Corneveaux, April N. Allen, Brian F. Porter, Jeremy J. Pruzin, Simon R. Platt, Marc Kent, and Matthew J. Huentelman

From the Department of Infectious Diseases, College of Veterinary Medicine, University of Georgia, Athens, GA (Barber); the Veterinary Emergency and Specialty Center of Santa Fe, Santa Fe, NM 87505 (Schatzberg); the Neurogenomics Division, Translational Genomics Research Institute, Phoenix, AZ (Corneveaux, Allen, Pruzin, and Huentelman); the Department of Veterinary Pathobiology, College of Veterinary Medicine and Biomedical Sciences, Texas A&M University, College Station, TX (Porter); and the Department of Small Animal Medicine and Surgery, College of Veterinary Medicine, University of Georgia, Athens, GA (Platt and Kent).

Address correspondence to Scott J. Schatzberg at the address above, or e-mail: scott.schatzberg@gmail.com

Abstract

Due to their unique population structure, purebred dogs have emerged as a key model for the study of complex genetic disorders. To evaluate the utility of a newly available high-density canine whole-genome array with >170 000 single nucleotide polymorphisms (SNPs), genome-wide association was performed on a small number of case and control dogs to determine disease susceptibility loci in canine necrotizing meningoencephalitis (NME), a disorder with known non-Mendelian inheritance that shares clinical similarities with atypical variants of multiple sclerosis in humans. Genotyping of 30 NME-affected Pug dogs and 68 healthy control Pugs identified 2 loci associated with NME, including a region within dog leukocyte antigen class II on chromosome 12 that remained significant after Bonferroni correction. Our results support the utility of this high-density SNP array, confirm that dogs are a powerful model for mapping complex genetic disorders and provide important preliminary data to support in depth genetic analysis of NME in numerous affected breeds.

Key words: *canine, genome-wide association, haplotype, major histocompatibility complex, necrotizing meningoencephalitis, single nucleotide polymorphism*

Necrotizing meningoencephalitis (NME) is an idiopathic inflammatory disorder of the central nervous system (CNS) that primarily affects young to middle aged toy breed dogs (Cordy and Holliday 1989; Stalis et al. 1995; Higgins et al. 2008). Inflammation in NME is characterized by mixed mononuclear cell infiltrates within the cerebral hemispheres and cortical leptomeninges with common clinical signs including seizures, depression, behavior change, circling, and visual deficits (Cordy and Holliday 1989). Similar to severe non-prototypical forms of multiple sclerosis (MS) such as Marburg variant (Bradl and Lassmann 2009; Hu and Lucchinetti 2009), NME is overrepresented in females, is rapidly progressive, and often carries a grave prognosis despite aggressive immunosuppressive treatment (Greer et al. 2009, 2010). NME initially was identified in Pug dogs in the late 1960s (Cordy and Holliday 1989) and is known to have a strong familial association in this breed (Cordy and Holliday 1989; Greer et al. 2009). Studies of Pugs with NME suggest that there are likely multiple genes that contribute to disease phenotype (Greer et al. 2009) and a recent genome-wide study of simple tandem repeat markers in this breed identified regions of disease susceptibility within dog leukocyte antigen (DLA) class II, similar to major histocompatibility complex (MHC) loci previously identified in MS and other proposed autoimmune diseases (Greer et al. 2010).

Purebred dog populations provide a unique opportunity for mapping genetic traits and recent technological developments have made it possible to leverage dogs as a model for the study of human genetic disease (Wilbe et al. 2010). The extensive linkage disequilibrium within breeds allows successful genome-wide mapping of traits and disease risk using smaller numbers of cases and controls than typically are required in a human-based study (Sutter et al. 2004; Lindblad-Toh et al. 2005), and dogs and humans share similar physiology with over half of the known canine diseases having a similar phenotype to analogous human diseases (Ostrander and Kruglyak 2000). Significant

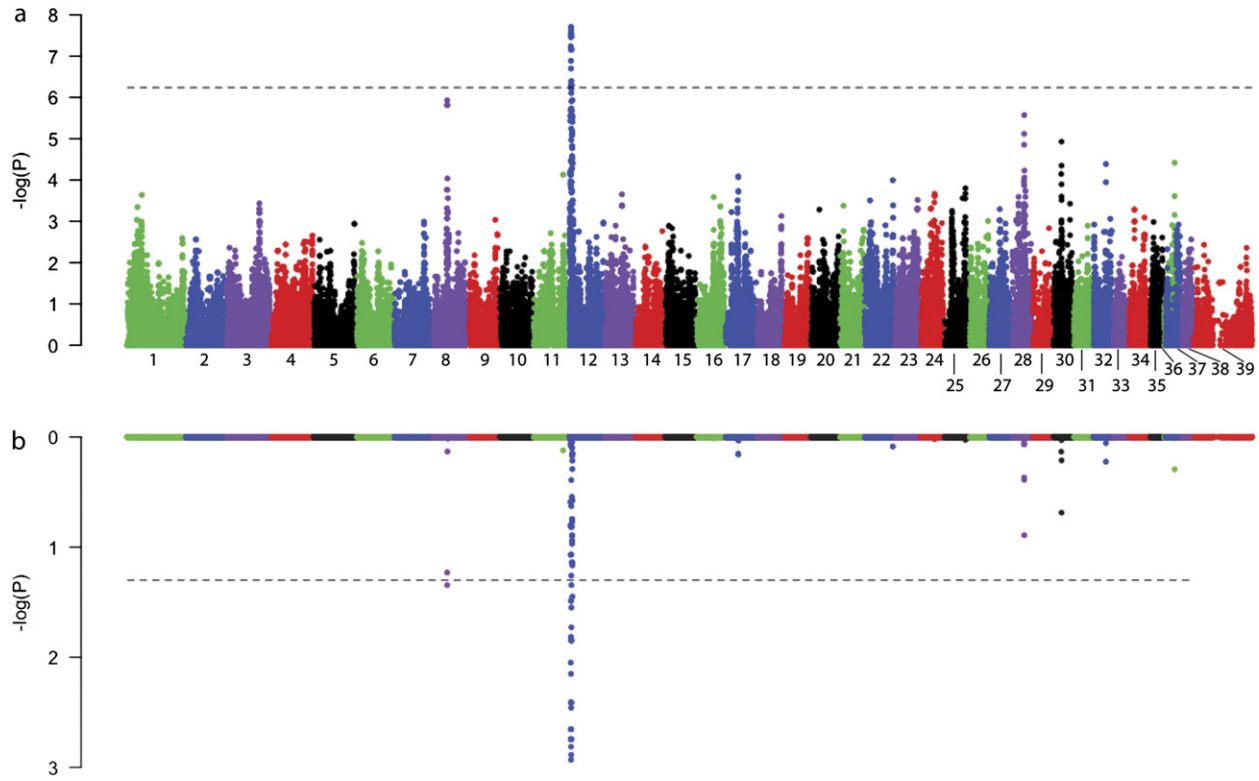

Figure 1. Genome-wide association results for 28 NME cases and 45 controls. (**a**) Fisher's exact tests were performed to compare SNP allele frequencies, and negative log *P* values were plotted across the genome. The horizontal dotted line represents the threshold for significant association after Bonferroni correction of $-\log(P) > 6.24$ with a strong peak on chromosome 12 maintaining genome-wide significance. (**b**) MaxT 100 000 permutation testing was performed, and negative log *P* values were plotted across the genome. The horizontal dotted line represents the threshold for significant association after permutation testing of $-\log(P) > 1.3$ with one SNP on chromosome 8 maintaining permuted significance.

advances in canine genomics, including publication of a high-quality draft genome sequence and identification of >2.5 million single nucleotide polymorphisms (SNPs), have facilitated mapping of simple and complex canine genetic traits (Lindblad-Toh et al. 2005; Karlsson et al. 2007; Wilbe et al. 2010), and genome-wide SNP arrays with coverage of up to 50 000 SNPs have been used successfully to map canine traits (Karlsson et al. 2007; Awano et al. 2009; Wilbe et al. 2010). The objective of this investigation was to employ a newly available high-density array to evaluate canine NME, a disorder with a presumed autoimmune etiology and complex mode of inheritance that has clinical similarities to atypical fulminant variants of MS. The identification of genetic risk factors should improve our understanding of NME pathophysiology, increase our ability to identify at risk and affected dogs, allow institution of targeted therapy, and ultimately may help in the identification of similar genetic factors that are associated with the development of rapidly progressive MS in people.

Materials and Methods

Study Population

Purebred Pug dogs were used for the case–control genome-wide association study. Cases were verified to have NME based on signalment, clinical history, and independent evaluation of hematoxylin and eosin brain sections by a veterinary neuropathologist. Cases ranged in age from 4 to 84 months (mean = 18 months, median = 26 months) and consisted of 11 males and 19 females. Control dogs had no evidence of neurological or autoimmune disease, ranged in age from 5 to 204 months (mean = 60 months, median = 48 months) at the time of sample collection, and consisted of 30 males and 38 females. Control dogs were followed for 18 months after sample collection to verify that they did not develop neurological or autoimmune disease.

SNP Genotyping

Genomic DNA was isolated using the Qiagen (Valencia, CA) Gentra Puregene Tissue Kit or Qiagen DNeasy Blood and Tissue Kit. SNP genotyping was performed with the Illumina (San Diego, CA) CanineHD Genotyping BeadChip using the Illumina BeadArray reader following the manufacturer's protocol (Stein et al. 2010).

Statistical Analysis

Genotyping was performed on 98 dogs, including 30 NME cases and 68 controls. Genome-wide analysis was performed

Table 1 SNPs with genome-wide significance after Bonferroni correction

Canine SNP	Chr	Pos	A_R/A_{NR}	F_A/F_U	P_{raw}	P_{genome}	OR (95% CI)	Gene
CF2P178662	12	5166878	A/G	0.95/0.52	2.36×10^{-8}	0.0020	16.1 (4.7–55.5)	*RT1-Db2*
BICF2S23225431	12	5217389	G/A	0.86/0.36	2.87×10^{-9}	0.0002	10.5 (4.4–25)	*RT1-Db2*
BICF2P22942	12	5227499	G/A	0.86/0.36	2.87×10^{-9}	0.0002	10.5 (4.4–25)	*RT1-Db2*
BICF2P194998	12	5275229	A/T	0.79/0.30	8.59×10^{-9}	0.0007	8.7 (4–19.2)	
rs8856588	12	5622709	C/A	0.79/0.30	8.59×10^{-9}	0.0007	8.7 (4–19.2)	*COL11A2*
BICF2P574765	12	5710832	A/G	0.79/0.30	8.59×10^{-9}	0.0007	8.7 (4–19.2)	*bing4-a*
BICF2P1186632	12	5734305	A/G	0.79/0.29	7.24×10^{-9}	0.0006	8.9 (4.1–19.7)	*TAPBP*
BICF2P1185629	12	5791672	G/A	0.79/0.30	8.59×10^{-9}	0.0007	8.7 (4–19.2)	*KIFC1*
BICF2P540937	12	5829667	A/G	0.79/0.32	6.27×10^{-8}	0.0054	7.9 (3.6–17.1)	*CUTA*
rs9189886	12	5843592	G/C	0.93/0.51	5.95×10^{-8}	0.0052	12.4 (4.1–37.3)	*Syngap1*
rs9006653	12	5916360	A/G	0.79/0.33	8.07×10^{-8}	0.0070	7.5 (3.4–16.2)	*Ppdpfb*
BICF2P1200278	12	5931001	G/A	0.79/0.29	7.24×10^{-9}	0.0006	8.9 (4.1–19.7)	*Ppdpfb*
rs9125534	12	5935549	A/G	0.79/0.30	8.59×10^{-9}	0.0007	8.7 (4–19.2)	*Ppdpfb*
BICF2S23322760	12	5992526	A/G	0.79/0.30	8.59×10^{-9}	0.0007	8.7 (4–19.2)	*Ppdpfb*
rs8760645	12	6024841	T/A	0.79/0.30	8.59×10^{-9}	0.0007	8.7 (4–19.2)	*Ppdpfb*
rs9245050	12	6028685	G/A	0.79/0.30	8.59×10^{-9}	0.0007	8.7 (4–19.2)	*Ppdpfb*
BICF2P863589	12	6059850	A/G	0.88/0.47	4.83×10^{-7}	0.0419	8 (3.3–19.7)	*Ppdpfb*
BICF2P1115728	12	6064245	C/A	0.88/0.47	4.83×10^{-7}	0.0419	8 (3.3–19.7)	*Ppdpfb*
BICF2P1254053	12	6149213	G/A	0.84/0.35	7.23×10^{-9}	0.0006	9.6 (4.2–22.2)	*MLN*
BICF2P402427	12	6160615	A/C	0.79/0.30	8.59×10^{-9}	0.0007	8.7 (4–19.2)	*Ggnbp1*
rs8694179	12	6164202	A/G	0.84/0.35	7.23×10^{-9}	0.0006	9.6 (4.2–22.2)	*Ggnbp1*
BICF2P459960	12	6184107	G/A	0.84/0.35	7.23×10^{-9}	0.0006	9.6 (4.2–22.2)	*Ggnbp1*
BICF2S22951431	12	6197313	A/C	0.79/0.30	8.59×10^{-9}	0.0007	8.7 (4–19.2)	*Ggnbp1*
BICF2P1261424	12	6200280	G/A	0.84/0.35	7.23×10^{-9}	0.0006	9.6 (4.2–22.2)	*Ggnbp1*
rs9120943	12	6218850	A/G	0.84/0.35	7.23×10^{-9}	0.0006	9.6 (4.2–22.2)	
rs9077055	12	6238545	A/G	0.84/0.35	7.23×10^{-9}	0.0006	9.6 (4.2–22.2)	
rs8677516	12	6257019	G/A	0.86/0.36	2.87×10^{-9}	0.0002	10.5 (4.4–25)	
BICF2P608380	12	6289014	G/A	0.86/0.36	2.87×10^{-9}	0.0002	10.5 (4.4–25)	
rs9132539	12	6299459	A/G	0.79/0.30	1.96×10^{-8}	0.0017	8.5 (3.9–18.6)	
BICF2P1340012	12	6311277	C/A	0.79/0.30	8.59×10^{-9}	0.0007	8.7 (4–19.2)	
BICF2P1211546	12	6320910	A/G	0.79/0.30	8.59×10^{-9}	0.0007	8.7 (4–19.2)	
BICF2P738783	12	6342204	A/C	0.79/0.29	6.06×10^{-9}	0.0005	9.2 (4.1– 20.3)	*LOC1127664*
BICF2P1313789	12	6653816	A/G	0.79/0.34	1.89×10^{-9}	0.0163	7.1 (3.3–15.4)	*NUDT3*
BICF2P1380652	12	6809061	A/G	0.79/0.33	8.07×10^{-8}	0.0070	7.5 (3.4–16.2)	*SPDEF*
BICF2P1462329	12	6832252	A/G	0.79/0.33	8.07×10^{-8}	0.0070	7.5 (3.4–16.2)	*SPDEF*

Chr, chromosome; Pos, physical position; A_R, risk allele; A_{NR}, nonrisk allele; F_A, allele frequency in cases; F_U, allele frequency in controls; and OR, odds ratio.

with PLINK (Purcell et al. 2007). Concordance on duplicate samples was 99.96%. Only samples with a call rate of >95% were included, resulting in analysis of 28 NME cases and 66 controls. A total of 172 115 SNPs were genotyped. Classic multidimensional scaling (Purcell et al. 2007) using a call rate of >97% and minor allele frequency (MAF) of >0.10 was performed on 85 366 SNPs to determine population stratification, and 21 controls that were not clustered with the main population of dogs were excluded resulting in a final population of 28 NME cases and 45 controls for analysis. These 45 control dogs ranged in age from 5 to 204 months (mean = 80 months, median = 48 months). Prior to analysis, 7324 SNPs were excluded for failure to reach the call rate threshold (>95%), and 81 001 SNPs were excluded for failure to reach the MAF threshold (>0.05). In total, 86 692 SNPs were used for analysis. Bonferroni correction was applied to account for multiple hypothesis testing with a resulting P value of 5.77×10^{-7} across 86 692 SNPs for genome-wide significance. To further evaluate genome-wide significance MaxT permutation testing (Purcell et al. 2007) of 100 000 permutations was applied.

Results

Initial genotyping was performed on 30 NME cases and 68 controls across 172 115 SNPs. After quality filtering and exclusion of population outliers (Supplementary Material, Supplementary Figure S1), analysis of 28 NME cases and 45 controls across 86 692 SNPs identified 2 disease-associated loci that reached genome-wide significance with correction for multiple hypothesis testing. The strongest association was on chromosome 12 where 35 SNPs within the DLA class II region reached genome-wide significance after Bonferroni correction (raw P value for Bonferroni genome-wide significance $< 5.77 \times 10^{-7}$) with the highest SNP having an odds ratio of 16.1 (95% confidence interval [CI]: 4.7–55.5) (Figure 1a and Table 1). Permutation testing using

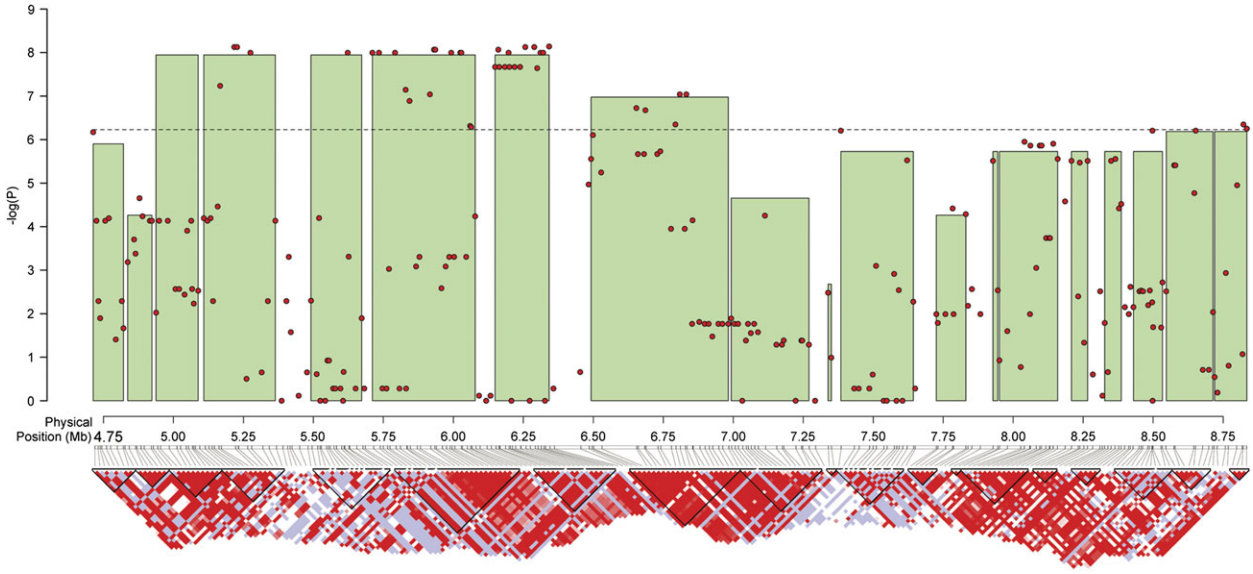

Figure 2. Haplotype analysis of NME-associated DLA II locus on chromosome 12. A 4.1 Mb region located from positions 4713392 to 8834652 is shown with 19 haplotype blocks generated in Haploview (Gabriel et al. 2002). Negative log *P* values from single SNP associations were derived from genome-wide analysis after removal of population outliers, and individual SNPs were plotted as red circles. The horizontal dotted line represents the threshold for significant association after Bonferroni correction of $-\log(P) > 6.24$.

100 000 permutations identified an additional 4 SNPs that reached genome-wide permuted significance within the DLA II locus and a second region of significance within the *STYX* gene on chromosome 8 ($P_{raw} = 2.11 \times 10^{-6}$, $P_{permuted} = 0.045$) with an odds ratio of 5.9 (95% CI: 2.7–12.5) (Figure 1b and Supplementary Material, Supplementary Table S1). To account for the fact that several of the control dogs were younger than the mean age of disease onset at the time of sample acquisition, the data were reanalyzed excluding all control dogs less than 24 months of age. Both the DLA and chromosome 8 regions remained significant with Bonferroni correction and permutation testing, respectively, but the significance was not improved by this exclusion (data not shown).

Haplotype analysis using Haploview (Barrett et al. 2005) identified 19 haplotype blocks across a 4.1 Mb region of DLA II on chromosome 12, all of which were associated with an increased risk for developing NME with *P* values ranging from 2.1×10^{-3} to 1.13×10^{-8} (Figure 2 and Supplementary Material, Supplementary Table S2). Manually forcing all of these haplotype blocks into a single haplotype resulted in the creation of a 4.1 Mb haplotype containing 241 SNPs. This haplotype was common and strongly associated with an increased risk of developing NME (case frequency 85.1%, control frequency 38.4%, $P = 7.97 \times 10^{-7}$). Haplotype analysis of the *STYX* region of chromosome 8 identified 4 haplotypes (Figure 3). The most significantly associated and common haplotype spanned the *STYX* and *GNPNAT1* genes and was protective based on phenotype ($P = 1.43 \times 10^{-6}$) (Supplementary Material, Supplementary Table S3). This block also contained 2 additional haplotypes significantly associated with NME risk ($P \sim 0.005$, data not shown).

Discussion

Genome-wide analysis of NME in Pug dogs identified 2 disease-associated loci, including a strong association with DLA II. Although recognition of self-antigen has not been demonstrated definitively as a mechanism of pathogenesis in NME, CNS anti-astrocytic antibodies have been identified (Toda et al. 2007), and the strong DLA II association further supports an autoimmune etiology. Similar to our findings in NME, most autoimmune diseases are polygenic with MHC II polymorphisms having the strongest disease association (Lincoln et al. 2005). Haplotype analysis of the DLA II region identified a large common block strongly associated with altered disease risk. The large number of genes present within this haplotype precludes the precise identification of the associated gene without additional fine mapping and sequencing of this region. Although initially described in the Pug, NME has now been described in numerous other breeds including the Maltese (Stalis et al. 1995) and Chihuahua (Higgins et al. 2008) with identical clinical presentation and pathology suggesting a similar etiopathogenesis among these breeds (Stalis et al. 1995; Higgins et al. 2008). Fine mapping across breeds should allow identification of smaller disease-associated haplotypes in this region (Karlsson et al. 2007; Parker et al. 2007).

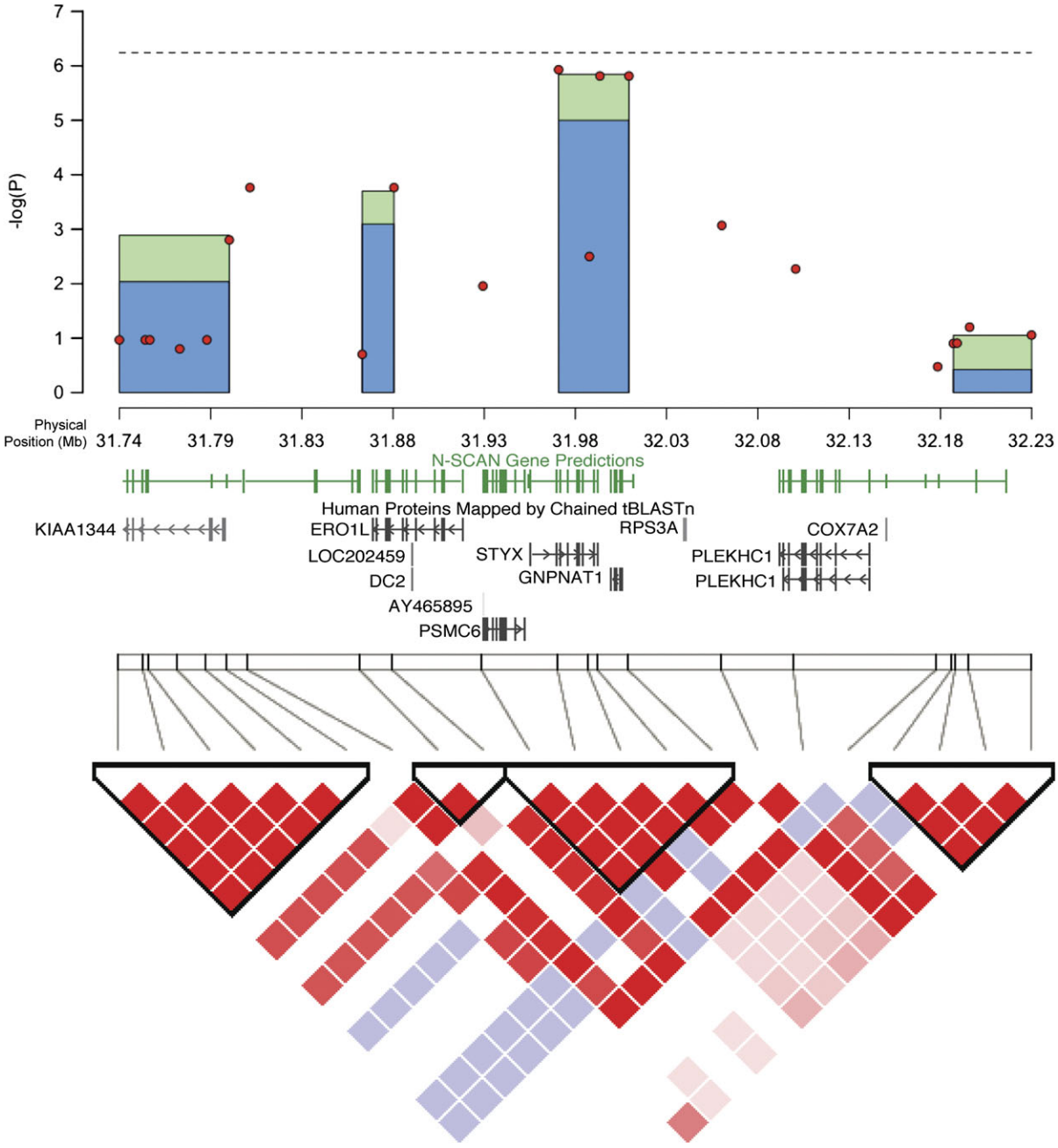

Figure 3. Haplotype analysis of NME-associated locus on chromosome 8. A 488 kb region located from positions 31736206 to 32225068 is shown with 4 haplotype blocks generated in Haploview (Gabriel et al. 2002). Negative log *P* values from single SNP associations were derived from genome-wide analysis after removal of population outliers, and individual SNPs were plotted as red circles. The horizontal dotted line represents the threshold for significant association after Bonferroni correction of $-\log(P) > 6.24$. The additional blue region within each haplotype block represents MaxT 100 000 permuted haplotypes.

The role of STYX and GNPNAT1 in NME also require further characterization. STYX, serine/threonine/tyrosine interacting protein, is a pseudophosphatase that lacks intrinsic catalytic activity and is structurally similar to members of the dual-specificity phosphatase subfamily of protein tyrosine phosphatases (Wishart et al. 1995). The only documented role of STYX is in normal sperm formation in mice (Wishart and Dixon 2002). The STYX protein has been found in numerous tissues in mice including brain (Wishart et al. 1995), but its presence and role in immune cells have not been determined. Protein tyrosine phosphatases play a key role in immune system function including lymphocyte

activation, with mutations in *PTPN22* having been documented in association with autoimmunity (Vang et al. 2005). Less is known about the role of pseudophosphatases in immune and inflammatory responses, although a mutation in the pseudophosphatase *MTMR13* has been implicated in a form of Charcot–Marie–Tooth neuropathy (Laporte et al. 2003), documenting a role for these proteins in development and maintenance of nervous tissue. STYX also is known to bind to the calcineurin substrate CRHSP-24 (Wishart and Dixon 2002). Although calcineurin plays an important documented role in T cell activation, the role of CRHSP-24 is less clear. CRHSP-24 has been found ubiquitously in rat tissue, and its dephosphorylation is prevented by administration of the immunomodulatory drugs cyclosporine and FK506 (Groblewski et al. 1998). Interestingly, CRHSP-24 has a brain-specific paralog, PIPPin, although interactions between STYX and PIPPin have not been documented (Wishart and Dixon 2002).

GNPNAT1, glucosamine-phosphate *N*-acetyltransferase 1, is involved in amino sugar metabolism including the formation of uridine diphospho-*N*-acetylglucosamine (UDP-GlcNAc). UDP-GlcNAc is an important cellular metabolite necessary for the synthesis of chitin, glycosylphosphatidylinositol protein anchors, and *N*-linked and *O*-linked glycans (Hurtado-Guerrero et al. 2007). *N*- and *O*-glycans play a documented role in normal thymic T-cell apoptosis (Earl et al. 2010), disruption of which could be speculated to lead to aberrant immune responses in NME.

The utility of dogs for the study of genetic traits has been recognized in recent years (Ostrander and Kruglyak 2000). Many common human diseases have a complex mode of inheritance, but responsible genes have remained elusive despite advances in the field of genomics (Eichler et al. 2010). The striking similarity of many naturally occurring canine diseases with specific human diseases suggests that risk genes and mechanistic pathways identified in dogs could be applied to advance our knowledge of human disease. The availability of ever improving technologies for the study of canine genomics makes such comparative studies possible. This investigation evaluated a new genome-wide SNP array with a significantly greater density than previously available arrays (averaging greater than 70 SNPs per Mb). The study confirmed the utility of this array, identifying disease-associated loci in less than 50 cases and 50 controls. Importantly, an unexpected amount of genetic variability existed within the purebred population of dogs evaluated here, requiring a large number of control dogs to be excluded from the study. These results highlight the importance of testing for population stratification even among canine breed populations that are assumed to be relatively homogeneous (Quignon et al. 2007).

In conclusion, evaluation of a canine CNS inflammatory disease that shares similarities with atypical severe forms of MS identified 2 important loci associated with disease development. Identification of these loci is an important step in elucidating the pathogenesis of NME. Further structural and functional analysis of the identified loci should improve the global understanding of idiopathic CNS inflammation and may aid in the development of improved diagnostics and treatments for dogs that suffer from this devastating disorder. Moreover, this information may help identify key genetic risk factors in atypical variants of MS.

Supplementary Material

Supplementary material can be found at http://www.jhered.oxfordjournals.org/.

Funding

Illumina, Inc.; Pug Dog Club of America; Morris Animal Foundation (D10CA-406); and American Kennel Club Canine Health Foundation (01455).

Acknowledgments

The authors thank the Pug owners, breeders, veterinarians, and breed clubs that contributed samples and supported completion of this investigation. This work was presented in part at the Fifth International Conference: Advances in Canine and Feline Genomics and Inherited Diseases, Baltimore, MD, 22–25 September 2010.

References

Awano T, Johnson GS, Wade CM, Katz ML, Johnson GC, Taylor JF, Perloski M, Biagi T, Baranowska I, Long S, et al. 2009. Genome-wide association analysis reveals a SOD1 mutation in canine degenerative myelopathy that resembles amyotrophic lateral sclerosis. Proc Natl Acad Sci U S A. 106:2794–2799.

Barrett JC, Fry B, Maller J, Daly MJ. 2005. Haploview: analysis and visualization of LD and haplotype maps. Bioinformatics. 21:263–265.

Bradl M, Lassmann H. 2009. Progressive multiple sclerosis. Semin Immunopathol. 31:455–465.

Cordy DR, Holliday TA. 1989. A necrotizing meningoencephalitis of pug dogs. Vet Pathol. 26:191–194.

Earl LA, Bi S, Baum LG. 2010. N- and O-glycans modulate galectin-1 binding, CD45 signaling, and T cell death. J Biol Chem. 285:2232–2244.

Eichler EE, Flint J, Gibson G, Kong A, Leal SM, Moore JH, Nadeau JH. 2010. Missing heritability and strategies for finding the underlying causes of complex disease. Nat Rev Genet. 11:446–450.

Gabriel SB, Schaffner SF, Nguyen H, Moore JM, Roy J, Blumenstiel B, Higgins J, DeFelice M, Lochner A, Faggart M, et al. 2002. The structure of haplotype blocks in the human genome. Science. 296:2225–2229.

Greer KA, Schatzberg SJ, Porter BF, Jones KA, Famula TR, Murphy KE. 2009. Heritability and transmission analysis of necrotizing meningoencephalitis in the Pug. Res Vet Sci. 86:438–442.

Greer KA, Wong AK, Liu H, Famula TR, Pedersen NC, Ruhe A, Wallace M, Neff MW. 2010. Necrotizing meningoencephalitis of Pug dogs associates with dog leukocyte antigen class II and resembles acute variant forms of multiple sclerosis. Tissue Antigens. 76:110–118.

Groblewski GE, Yoshida M, Bragado MJ, Ernst SA, Leykam J, Williams JA. 1998. Purification and characterization of a novel physiological substrate for calcineurin in mammalian cells. J Biol Chem. 273:22738–22744.

Higgins RJ, Dickinson PJ, Kube SA, Moore PF, Couto SS, Vernau KM, Sturges BK, Lecouteur RA. 2008. Necrotizing meningoencephalitis in five Chihuahua dogs. Vet Pathol. 45:336–346.

Hu W, Lucchinetti C. 2009. The pathological spectrum of CNS inflammatory demyelinating diseases. Semin Immunopathol. 31:439–453.

Hurtado-Guerrero R, Raimi O, Shepherd S, van Aalten DMF. 2007. Glucose-6-phosphate as a probe for the glucosamine-6-phosphate N-acetyltransferase Michaelis complex. FEBS Lett. 581:5597–5600.

Karlsson EK, Baranowska I, Wade CM, Salmon Hillbertz NHC, Zody MC, Anderson N, Biagi TM, Patterson N, Pielberg GR, Kulbokas Iii EJ, et al. 2007. Efficient mapping of mendelian traits in dogs through genome-wide association. Nat Genet. 39:1321–1328.

Laporte J, Bedez F, Bolino A, Mandel J-L. 2003. Myotubularins, a large disease-associated family of cooperating catalytically active and inactive phosphoinositides phosphatases. Hum Mol Genet. 12:R285–R292.

Lincoln MR, Montpetit A, Cader MZ, Saarela J, Dyment DA, Tisslar M, Ferretti V, Tienari PJ, Sadovnick AD, Peltonen L, et al. 2005. A predominant role for the HLA class II region in the association of the MHC region with multiple sclerosis. Nat Genet. 37:1108–1112.

Lindblad-Toh K, Wade CM, Mikkelsen TS, Karlsson EK, Jaffe DB, Kamal M, Clamp M, Chang JL, Kulbokas EJ, Zody MC, et al. 2005. Genome sequence, comparative analysis and haplotype structure of the domestic dog. Nature. 438:803–819.

Ostrander EA, Kruglyak L. 2000. Unleashing the canine genome. Genome Res. 10:1271–1274.

Parker HG, Kukekova AV, Akey DT, Goldstein O, Kirkness EF, Baysac KC, Mosher DS, Aguirre GD, Acland GM, Ostrander EA. 2007. Breed relationships facilitate fine-mapping studies: a 7.8-kb deletion cosegregates with Collie eye anomaly across multiple dog breeds. Genome Res. 17: 1562–1571.

Purcell S, Neale B, Todd-Brown K, Thomas L, Ferreira MAR, Bender D, Maller J, Sklar P, de Bakker PIW, Daly MJ, et al. 2007. PLINK: a tool set for whole-genome association and population-based linkage analyses. Am J Hum Genet. 81:559–575.

Quignon P, Herbin L, Cadieu E, Kirkness EF, Hédan B, Mosher DS, Galibert F, André C, Ostrander EA, Hitte C. 2007. Canine population structure: assessment and impact of intra-breed stratification on SNP-based association studies. PLoS One. 2:e1324.

Stalis IH, Chadwick B, Dayrell-Hart B, Summers BA, Van Winkle TJ. 1995. Necrotizing meningoencephalitis of Maltese dogs. Vet Pathol. 32:230–235.

Stein JL, Hua X, Morra JH, Lee S, Hibar DP, Ho AJ, Leow AD, Toga AW, Sul JH, Kang HM, et al. 2010. Genome-wide analysis reveals novel genes influencing temporal lobe structure with relevance to neurodegeneration in Alzheimer's disease. Neuroimage. 51:542–554.

Sutter NB, Eberle MA, Parker HG, Pullar BJ, Kirkness EF, Kruglyak L, Ostrander EA. 2004. Extensive and breed-specific linkage disequilibrium in Canis familiaris. Genome Res. 14:2388–2396.

Toda Y, Matsuki N, Shibuya M, Fujioka I, Tamahara S, Ono K. 2007. Glial fibrillary acidic protein (GFAP) and anti-GFAP autoantibody in canine necrotising meningoencephalitis. Vet Rec. 161:261–264.

Vang T, Congia M, Macis MD, Musumeci L, Orru V, Zavattari P, Nika K, Tautz L, Tasken K, Cucca F, et al. 2005. Autoimmune-associated lymphoid tyrosine phosphatase is a gain-of-function variant. Nat Genet. 37:1317–1319.

Wilbe M, Jokinen P, Truve K, Seppala EH, Karlsson EK, Biagi T, Hughes A, Bannasch D, Andersson G, Hansson-Hamlin H, et al. 2010. Genome-wide association mapping identifies multiple loci for a canine SLE-related disease complex. Nat Genet. 42:250–254.

Wishart MJ, Denu JM, Williams JA, Dixon JE. 1995. A single mutation converts a novel phosphotyrosine binding domain into a dl-specificity phosphatase. J Biol Chem. 270:26782–26785.

Wishart MJ, Dixon JE. 2002. The archetype STYX/dead-phosphatase complexes with a spermatid mRNA-binding protein and is essential for normal sperm production. Proc Natl Acad Sci U S A. 99:2112–2117.

Received November 10, 2010; Revised March 16, 2011; Accepted April 27, 2011

Corresponding Editor: John Fyfe